BBAA VI International Colloquium on:
Bluff Bodies Aerodynamics & Applications
Milano, Italy, July, 20-24 2008

LES OF FLOWS AROUND A CIRCULAR CYLINDER IN THE CRITICAL REYNOLDS NUMBER REGION

Yoshiyuki ONO[*], Tetsuro Tamura [†]

[*] *Fluid Engineering Department, Technical Research Institute, Obayashi Corporation*
4-640 Simokiyoto, Kiyose, Tokyo, Japan, ono.yoshiyuki@obayashi.co.jp
[†] *Department of Environmental Science and Technology, Tokyo Institute of Technology*
4259 Nagatsuta, Midori-ku, Yokohama, Japan, tamura@depe.titech.ac.jp

Keywords: LES, Circular cylinder, The critical Reynolds-number region, Vortex structure

1 INTRODUCTION

The recent advancement of numerical techniques has made it possible to easily simulate the flow around bluff body. Some LES methods succeed in simulating the large scale wake structures associated with the flow separation on a circular cylinder at sub-critical Reynolds numbers. On the other hand, in the critical Reynolds number region, the flow represents an intricate combination of laminar separation, transition, reattachment and turbulent separation of the boundary layers on the cylinder [1]-[4]. This difference between the flow characteristics in the sub-critical and the critical Reynolds number regions results in discontinuous drop of the drag and jump in vortex shedding frequency.

Until now, many numerical models have been applied to the thus complicated flow in the critical Reynolds number region. However, the previous LES computations show an ambiguous decrease of the drag coefficient and an insufficient increase of vortex shedding frequency in comparison with the experiments, mainly due to too much numerical dissipation. Furthermore, the details of the complicated flow structure in the critical region have never been numerically captured.

In this research, we introduce sophisticated numerical model. Also especially focusing on the complicated flow structure near the flow separation region, the flow around a circular cylinder at very high Reynolds number ($Re=6\times10^5$) is investigated by using LES method. First, the adequate numerical model is investigated. The influences of (1) the numerical dissipation, (2) SGS model and (3) grid resolution on the aerodynamic quantities are examined. Next, the computed flow structure are investigated

2 PROBLEM FORMULATION

The governing equations are given by the incompressible Navier-Stokes and the continuity equations. To advance the solutions of velocities and pressure in time, a fractional step method is employed. The time integral of the momentum equation is hybrid, that is to say, the

Crank-Nicolson scheme is applied to the viscous terms and the explicit third-order Runge-Kutta method is used for convective terms. Spatial derivatives of variables are treated as second-order central difference. Convective terms are approximated using the higher-order interpolation method. To avoid the numerical oscillation, very slight numerical dissipation is added to convective terms by controlling numerical dissipation parameter. To study the effect of SGS model, the dynamic Smagorinsky model and the dynamic mixed model are used.

3 COMPUTATIONAL MODEL

In order to distribute the grid points in the whole domain around a circular cylinder with a balanced size, the over-set grid system is employed. Figure1 shows the overset grid system near the cylinder in the present computations which is composed by three kinds of meshes. 2D length in the span-wise direction is used. In order to investigate the influence of the grid-resolution, the computations are carried out using three types of grids. The grid points in the each Grid are shown in table 1. Grid 2 and grid 3 have finer grid resolutions in the azimuth direction and the span-wise direction, respectively.

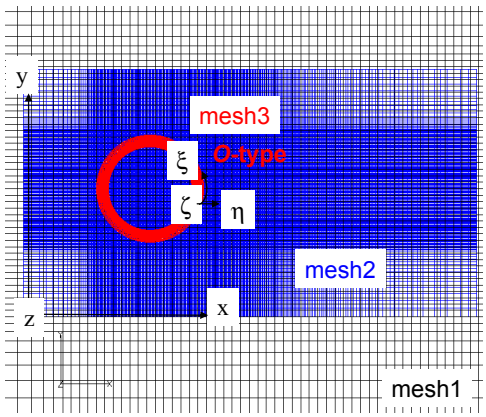

Figure 1 Overset grid system

Table 1 Computational grid points

Grid	Dir	Mesh1	Mesh2	Mesh3
Grid1	x(ξ)	101	311	501
	y(η)	91	181	61
	z(ζ)	31	51	51
Grid2	x(ξ)	101	311	801
	y(η)	91	181	61
	z(ζ)	31	51	51
Grid3	x(ξ)	101	311	501
	y(η)	91	181	61
	z(ζ)	31	151	151

4 COMPUTAIONAL RESULTS

4.1 Influence of numerical conditions

The computed aerodynamic quantities such as time-averaged drag coefficient, the r.m.s value of the fluctuations lift coefficients and the Strouhal numbers are summarized in Table 2. Concerning the effects of the size of the numerical dissipation, the calculations including large numerical dissipation (α=0.2) produces higher value of time-averaged drag coefficient than the other cases. In the case using smaller than α=0.05, the computations became unstable, and overflowed. In the present numerical conditions, there is a little effect of the SGS models and the grid resolution in azimuth direction on the aerodynamic characteristics. Also, the cases using Grid1 and Grid2 couldn't accurately predict an increase of the Strouhal number in the critical region [2]-[4]. On the other hand, the calculation using finer grid resolution in the span-wise direction simulates an increase of the Strouhal number and a decrease of the C_D, observed in the previous experiments [2]-[4]. Consequently, grid resolution in the span-wise direction is very important to simulate the flow around a circular cylinder in the critical region. In next section, based on the computations using grid 3, the details of the flow around a circular cylinder in the critical region are studied.

4.2 Study of averaged flow

Figure 2 and Figure 3 show the time-averaged stream-wise velocities close to the cylinder surface and the time-averaged pressure distributions on the cylinder. The stream-wise velocity shows the negative value at around 100 degree and then changes to the positive value associated with the flow separation and the flow reattachment to the cylinder. Concerning the pressure characteristics, the flat distributions are recognized in around 100 degree and the rear side of 140 degree associated with the flow separation and the re-separation. Looking at the upstream flat region, the computed length of the flat region associated with the time averaged size of separation bubbles shows agreement with the experiments by Flachsbart [4].

Table 2 Computed aerodynamic coeffucuents

Numerical condition			Computational results		
mesh	SGS model	α*	CD ave	CL rms	St
Grids1	DS	**0.2**	0.46	0.13	0.34
Grids1	DS	**0.1**	0.36	0.13	0.30
Grids1	DS	**0.05**	0.36	0.13	0.31
Grids1	**DM**	0.1	0.33	0.12	0.30
Grids1	**DM**	0.05	0.34	0.17	0.29
Grids2	DS	0.1	0.32	0.12	0.33
Grids2	DM	0.1	0.33	0.115	0.3
Grids3	DM	0.1	0.23	0.07	0.43
EXP [2]-[4]			**0.2-0.4**	**0.02-0.13**	**0.42-0.48**

* In the case of the UTOPIA scheme, α=1.0.

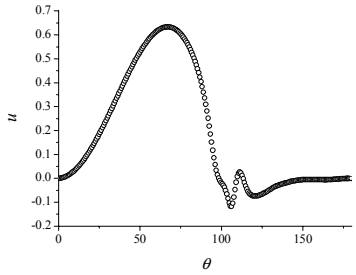

Figure 2 Time-averaged stream-wise velocity

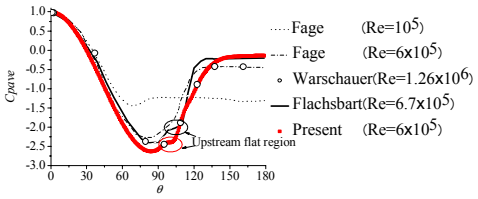

Figure 3 Time-averaged pressure coefficients

4.3 Study of instantaneous flow structure in the critical Reynolds number region

Figure 4 shows the contours of the stream-wise velocity around a circular cylinder. The very narrow near wake which results in a decrease of C_D and an increase of the St is recognized. Figure 5(1) shows the velocity vectors near the flow separation region. It can be seen that the separation-points of the flow randomly changes in the span-wise direction. Also, instantaneous reattachment and re-separation are observed in the rear side of the separation points. Figure 5(2), (3) show the iso-surfaces of pressure around a cylinder and the contours of vortices ωz close to a cylinder. Separation bubbles are also randomly distorted in the span-wise direction. The disruption and fragmentation of the separation bubbles are observed in the computations. According to the previous research by Bearman [2], 2D separation bubbles are stably formed after separation at the critical Reynolds number. But, the two-dimensionality is sensitively disrupted by small protrusion on cylinder surface such as a pressure tapping hole or dust particles. Also, some flow visualizations showed separation lines tend to be broken as Reynolds number increases in the critical region [4]. The present computation simulates these characteristics of separation bubble in the critical region. Furthermore, Figure 6 shows the comparison of the computed stream lines with the oil flow patterns in the experiments by Loiseau et al. [4]. The computed stream lines shows good agreement with the oil flow patterns in the previous experiments.

Figure 7 shows the iso-surface of stream-wise velocity (U=0.0) near the separation points. In the rear of the reattachment region, the development of boundary-layer turbulence along the cylinder surface, and turbulent separation on the cylinder are captured in the present computations.

5 CONCLUSIONHEADINGS

The LES method is applied to the flow around a circular cylinder at high Reynolds number. The LES model using very small numerical dissipation and fine grid resolution in the span-wise direction gives good results. The present computation succeeds in simulating the fragmentation of separation bubbles in the upper critical region observed in the previous experiments. In the rear of the reattachment region, the development of boundary-layer turbulence along the cylinder surface, and turbulent separation on the cylinder are simulated.

REFERENCES

[1] A., Fage, J.H., Warsap, The effects of turbulence and surface roughness on the drag of a circular cylinder, Aero.,Res.,Counc., Lond.,R and M Nov.1283,1929.

[2] P.W.,Bearman, On vortex shedding from a circular cylinder in the critical Reynolds number region. Journal Fluid Mechanics, 37, pp577-587, 1969.

[3] G., Schewe, On the force fluctuations acting on a circular cylinder in cross flow from subcritical up to transcritical Reynolds number, Journal Fluid mech., 133, 1983, pp265-286

[4] M.M. Zdravkovich, Flow around Circular Cylinders, Vol1, Oxford university press, 1997.

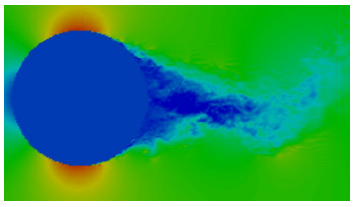

Figure 4 Contours of instantaneous velocity

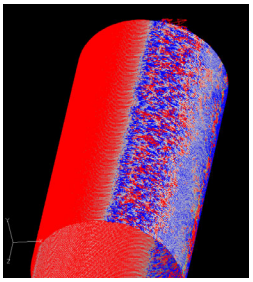

(1)Velocity vectors

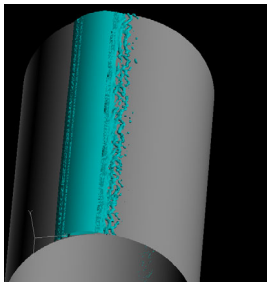

(2) Iso-surface of pressure

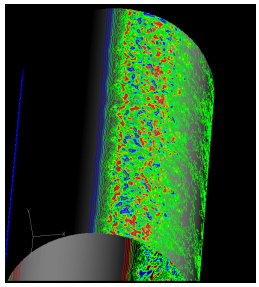

(3) Contours of vortices

Figure 5 Computed flow near the cylinder in the critical region

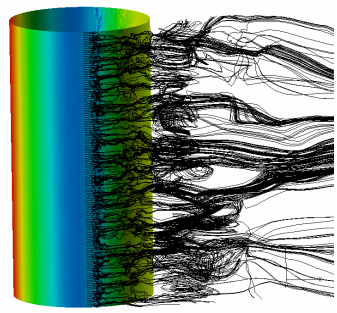

Computations

Oil flow patterns [4]

Figure 6 Stream lines

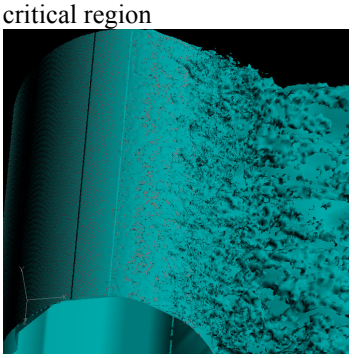

Figure 7 Iso-surface of the stream-wise velocity (u=0)